

# Comparison of Four Space Propulsion Methods for Reducing Transfer Times of Manned Mars Mission

André G. C. Guerra<sup>a,1</sup>, Orfeu Bertolami<sup>b</sup>, Paulo J. S. Gil<sup>c,\*</sup>

<sup>a</sup>Instituto Superior Técnico, Universidade de Lisboa, Av. Rovisco Pais, 1049-001 Lisboa, Portugal

<sup>b</sup>DFA, Faculdade de Ciências, Universidade do Porto, Rua do Campo Alegre 687, 4169-007 Porto, Portugal

<sup>c</sup>CCTAE, IDMEC, Instituto Superior Técnico, Universidade de Lisboa, Av. Rovisco Pais, 1049-001 Lisboa, Portugal

## Abstract

We assess the possibility of reducing the travel time of a manned mission to Mars by examining four different propulsion methods, and keeping the mass at departure under 2,500 tonnes, for a fixed architecture. We evaluated representative systems of three different state of the art technologies (chemical, nuclear thermal, and electric), and one advance technology, the “Pure Electro-Magnetic Thrust” (PEMT) concept (proposed by Rubbia). A mission architecture mostly based on the Design Reference Architecture 5.0 is assumed in order to estimate the mass budget, that influences the performance of the propulsion system. Pareto curves of the duration of the mission and time of flight versus mass of mission are drawn. We conclude that the ion engine technology, combined with the classical chemical engine, yields the shortest mission times for this architecture with the lowest mass, and that chemical propulsion alone is the best to minimise travel time. The results obtained using the PEMT suggest that it could be a more suitable solution for farther destinations than Mars.

**Keywords:** Manned Mission, Mars, Propulsion

## 1. Introduction

Interplanetary space travel takes a long time with current technology. For example, it takes many months to reach Mars, and a few years for a return mission [1, 2]. In the case of manned missions, such long travel times require huge life support systems (food, air, etc.) capable of enduring the harshness of the space environment for long periods. These long travel times also present other complications, e.g. health problems and an increased probability of solar storms during travel, which increases the risk to the astronauts life and to the success of the mission. These difficulties can be eventually minimised if the propulsion system used is powerful enough to significantly diminish both the travel time and the waiting time to return.

With the objective of evaluating the possibility of cutting short the total travel time of an interplanetary manned spacecraft, we compare the performance of different types of propulsion systems. We focus the analysis on a manned mission to Mars as it is the next natural step for human exploration of the solar system. A single mission architecture is used as the baseline, while different propulsion systems, in type and size, are tested to assess the impact on the duration of the mission. The mission architecture was selected in order to minimize mass (which means cost) but without using options such as in situ resource management or aerobraking that could increase the risk

of the mission. Assessment of other mission architectures to determine their impacts on mission durations was outside the scope of this study.

Historically, two main concepts for manned missions to Mars have received significant attention: Mars Direct and the Design Reference Mission.

Mars Direct was a mission developed by Robert Zubrin in 1990 [1]. The total mass was set to be below 1,000 t, which was regarded as a feasible technological limit by the author, and the technology restricted to what was available at the time. The proposal comprised two Saturn V type launchers, one bearing a 45 t unmanned cargo module and the other a 25 t human habitat module, with a crew of four astronauts. The modules used the chemical upper stage of the rockets to launch to a 180 day transfer to Mars. Upon arrival the modules were assumed to execute an aerocapture manoeuvre for capture into Mars orbit. For the return the crew used fuel produced from Mars’ atmosphere, and again a 180 day transfer back to Earth. In total, the mission would last 910 days, with an estimated cost of US \$25 billion in dollars of 1990.

The other concept, dubbed “Design Reference Mission” (DRM) was developed in 1992-1993, and was based on Mars Direct [2]. It has been revised several times, with the last version designated the Mars Design Reference Architecture (DRA) 5.0 [3]. It was assumed to comprise a crew of six astronauts, and transfers of about 180 days (for the crew). Together with a waiting time of about 500 days, the total mission would take around 900 days [3]. Moreover, a maximum of twelve Saturn V type launchers (the Ares V), bearing a descent/ascent vehicle (DAV), a surface habitat (SHAB) and a multi-module Mars transfer ve-

\*Corresponding author

Email addresses: aguerra@fc.up.pt (André G. C. Guerra), orfeu.bertolami@fc.up.pt (Orfeu Bertolami), p.gil@dem.ist.utl.pt (Paulo J. S. Gil)

<sup>1</sup>Present address: DFA, Faculdade de Ciências, Universidade do Porto, Rua do Campo Alegre 687, 4169-007 Porto, Portugal.

hicle (MTV), would be needed. Each module would use nuclear thermal rockets as propulsion system and would have a mass ranging between 60 tonne and 80 tonne.

Both proposals foresee an extended mission duration. It is well known that in space humans are subjected to many hazards, such as loss of bone/muscle mass and a substantial increase in the probability of developing cancer [4, 5]. Therefore, a 180 day transfer (plus waiting time and a similar time to return) is a significant risk, most particularly in view of the unpredictability of the solar cycle.

Other mission concepts were developed after those presented above, for example the “Austere Human Missions to Mars” [6]. These are variants of the DRM, with updated technology, but without considerable differences in the mission duration. Additionally, many concepts include insufficiently tested technologies, such as *in situ* resource utilisation or aerocapture, increasing the risks, cost, or the development time of the mission.

There are two key factors worth considering when trying to develop an architecture for human missions to Mars. Firstly, only the manned component of the system has a strong requirement to minimise travel time; accessories to be used later can be sent in advance and meet the astronauts afterwards, thus minimising cost. Secondly, mass is one of the drivers of the cost and performance of the system. Consequently, a spacecraft divided in modules, serving specific functions at specific phases, and discarded as soon as they have fulfilled their function can be used to minimise the total mass, following the successful lunar orbit rendezvous approach used in the Apollo project [7].

Therefore, our approach is to use a baseline mission architecture that fulfils all the major requirements of a manned mission to Mars, and minimises the mass launched from Earth by separating the manned part from the cargo component. Afterwards, we select four propulsion technologies for evaluation, and determine the minimum transfer time possible for the manned component, as a function of the size of the engines (respecting known engine size constraints). Selected propulsion technologies include: classical chemical engines (as it has been the workhorse of space exploration), nuclear thermal engines (which in the 1940s was believed to be the future technology for exploring the solar system), modern electrical engines (as it is currently considered the best flight proven system for many applications due to its high specific impulse), and a more conjectural concept of the many that have been proposed as the next revolutionary engine. We selected as the revolutionary engine the “Pure Electro-Magnetic Thrust” (PEMT) concept because it promised, in theory, to be highly effective due to its full conversion of mass into energy with momentum usable for thrust. We are interested in finding the minimum order of magnitude of the mission duration, within feasible bounds, and comparing the merits of the different propulsion systems. We have not optimised the mission for each propulsion system. We have instead considered only transfer trajectories that provide representative performance for each system.

## 2. Selected Propulsion Technologies

Many concepts for manned missions to Mars resort to chemical propulsion or nuclear thermal systems, but do not include the most advanced types of propulsion systems, including new chemical engines [8, 9, 10, 11, 12]. We have selected four examples of state of the art or advanced propulsion technologies, and evaluate their potential to reduce the duration of human Mars missions (similar to the DRA 5.0 architecture), respecting a reasonable criteria for the total mass of the mission ( $\leq 2,500$  t).

The selected propulsion systems exhibit high specific impulse ( $I_{sp}$ ), high thrust ( $F_T$ ) and high thrust-to-weight ratio ( $F_T/w$ ) among the numerous technologies available in the literature. We have considered propulsion technologies currently being tested or with flight proven capabilities. In addition, one propulsion system was examined that is an exception to this latter premise, the PEMT, presented by Carlo Rubbia [13]. For a broader discussion of propulsion systems, including a putative gravity control, the reader is referred to references [10, 14, 15, 16, 17].

The four propulsion systems considered are the:

1. Common Extensible Cryogenic Engine (CECE) – representing the classical chemical propulsion;
2. Nuclear Engine for Rocket Vehicle Application (NERVA) II – assumed to be representative of nuclear thermal propulsion technology;
3. Radio Frequency Ion Technology (RIT) XT – assumed to be representative of modern electric propulsion technology;
4. Pure Electro-Magnetic Thrust (PEMT) – an advanced concept propulsion concept.

### 2.1. Classical Chemical Engines

In this brief discussion we do not consider storable, monopropellant, or solid systems [9], but only cryogenic systems, due to their higher thrust (when compared to the aforementioned systems) and  $I_{sp} \approx 400$  s [10].

Chemical engines present high thrust and relatively low  $I_{sp}$ , and accelerating continuously with a chemical engine would rapidly lead to an impractical mass budget. They are therefore used as impulsive engines, i.e. only active for small intervals of time (and the spacecraft is in free fall for most of its trajectory). Nevertheless, chemical engines can be crucial in escape and capture manoeuvres, because of their high thrust. Furthermore, impulsive engines can minimise the so called gravity losses for the same total  $\Delta v$  available, by being used at once in a more favourable location [18] — usually deeper in the gravity well — and with the additional advantage of possibly dumping empty fuel tanks sooner, maximising performance.

The most important limitation of the chemical propulsion is that it is limited to the available chemical energy and thermodynamic conditions of the propellants [10]. The main point

of developing other propulsion methods is to overcome these limitations.

For our Mars mission, we only consider operations in space, taking for granted that some launch vehicle takes the system into orbit. An engine with the ability to be restarted is also required, to cope with the various mission phases. Examples of modern chemical engines fulfilling these criteria are the Vinci engine, that is being designed for the upper stage of Ariane 5 [19], the RL10B-2, the latest version of the RL 10 engine and used in the Delta IV launch vehicle [20], and the Common Extensible Cryogenic Engine (CECE) of Pratt & Whitney Rocketdyne [21], also an evolution of the RL 10. Of course, forthcoming technological developments involving, for instance, zero boil off for cryogenic propulsion fluids might be considered, but as most often these represent improvements rather than breakthroughs they will probably not affect considerably our assumptions and conclusions.

We selected as representative of the chemical propulsion system the CECE engine. Although the thrust of the Vinci engine (180 kN) is higher than the others ( $\approx 110$  kN), it has a much higher mass (almost the double of the lighter). Additionally, they all have similar  $I_{sp}$ . Consequently, the CECE has a much higher thrust-to-weight ratio, which, together with the ability to restart many more times (50, instead of 5 or 15), makes it the best choice for such a complex mission. Relevant characteristics of one CECE engine can be found in Table 1, where in all cases the mass of propellants and their deposits is not included since they can be discarded and will be accounted separately.

## 2.2. Nuclear Thermal Engines

Nuclear thermal engines have been developed since the 1940s, and were even considered for the upper stage on the Nova rocket (for the lunar direct launch mission) [10]. Their working principle is similar to chemical engines, with high thrust and  $I_{sp} \approx 800$  s, and therefore should be treated as impulsive. A single propellant, usually hydrogen, is heated by the nuclear core and is expelled through a nozzle while expanding. The core, usually an uranium derivative (like dioxide or carbide) or plutonium, releases heat due to the nuclear reaction, providing energy to the gas expansion, and resulting in an  $I_{sp}$  approximately the double of the chemical engines. The heat released is limited by the melting point of the materials [9].

One of the engines with highest power to be developed within the Nuclear Engine for Rocket Vehicle Application (NERVA) program was the NERVA II, which had the goal of achieving a higher  $I_{sp}$ , and thrust, with a lower weight than previous models [22]. It was intended to serve as the propulsion system for manned interplanetary missions with masses close to 1,000 t. NERVA II produced the required power with a uranium inventory of 360 kg, and had 2 m in diameter [22]. Temperatures of the hydrogen fuel could reach 2,755 K [22]. One of the requirements of the program was an endurance of over 600 min [24]. Its main features are shown in Table 1.

Another engine, with interesting features, developed within Project Rover program, was the Phoebus II engine, which featured  $F_T/w = 38$  and  $I_{sp} = 790$  s [25]. These values are a little

higher but the difference to NERVA II is not too large and this engine showed overheating problems during the tests conducted at the time.

Options such as the ORION, a nuclear pulse propulsion system developed in the 1950/1960s, was not considered due to its low  $F_T/w$  (between one and six), and the need to blast nuclear material [26]. Notice that even though the ORION proposal has a greater  $F_T/w$  than electric propulsion (discussed below), the  $I_{sp}$  of the latter is much larger than the former.

## 2.3. Modern Electric Engines

Electric propulsion overcomes the limitations of chemical engines by separating the energy source from the propellant material, and by not using thermodynamic mechanisms to accelerate particles. Common sources of energy are solar, nuclear power generation, and radioisotope thermal generators (RTG) [9]. The thrust produced by current technology is very small, when compared to chemical engines. However, they can achieve much larger  $I_{sp}$ , allowing the engine to run for longer periods with less fuel. The electric engine is treated as a non-impulsive engine since it is working most of the flight. In these systems we have to take into account not only the mass of the engine but also the mass of the associated energy system, e.g. solar panels and the power supply and control unit (PSCU) [27].

The selected power source is the solar photovoltaic, since nuclear power systems represent a large increase of the engine mass, and the RTG technology can only achieve specific powers of 5 W/kg (and are under development) [9]. The size and mass of the required solar array can be estimated for the power level of the engine used (as indicated in Table 1) [28], and must be taken into account on the mass budget of the mission. We considered an efficiency of 29.5% for the solar cells, a density of  $\rho_A^{sp} = 0.84$  kg/m<sup>2</sup>, with degradation rate of 0.4% per year, and the worst case scenario of a three-year mission [29, 28]. For the PSCU a direct-drive concept was used, with a corresponding mass given by a scaling parameter ( $M^{PSCU} = 0.35W + 1.9$  kg) [27]. These values give a density for the associated energy system of about 7 kg/kW, well within what was used in other studies [17].

Several electric propulsion technologies are in use such as the arcjet, Hall effect, and gridded ion thrusters [9]. Modern examples of electric engines are NASA's Evolutionary Xenon Thruster (NEXT), an evolution of the already tested NASA Solar Technology Application Readiness (NSTAR) used in the Deep Space 1 mission [30] and Dawn [31], the radio frequency ion thruster RIT-XT, which works by generating ions using high frequency electromagnetic fields and is very similar to the RIT-22 engine (in design and thrust-to-weight ratio) but has higher  $I_{sp}$  [23, 32], and the PPS 1350-G, which is a plasma thruster with flight proven capability (SMART-1 mission) [33].

To select the electric propulsion system, including all elements required such as power processing electronics and power source, we considered not only the specific impulse  $I_{sp}$  but also the thrust-to-weight ratio, because the latter also affects the transfer time [34], which is our main concern. Moreover, the power requirements of the engine also influence the engine selection, since it has an impact on the size and mass of the

Table 1: Main characteristics of selected engines for a system consisting of one engine (data from [21, 22, 23]). The mass of propellants and their deposits is not included

Engine	Power [W]	$I_{sp}$ [s]	Thrust [N]	Mass [kg]	$F_T/w$ [N/kg]
CECE	-	465	$0.11 \times 10^6$	256	435
NERVA II	$5.0 \times 10^9$	785	$1.0 \times 10^6$	$34 \times 10^3$ <sup>a</sup>	30
RIT-XT	3,260	4,600	0.12	32 <sup>b</sup>	$3.7 \times 10^{-3}$
PEMT	$6.1 \times 10^9$	$30.6 \times 10^3$	20	$32 \times 10^3$ <sup>c</sup>	$0.64 \times 10^{-3}$

<sup>a</sup> The reactor's mass is  $11 \times 10^3$  kg.

<sup>b</sup> Includes mass of the required solar panels and power processing electronics.

<sup>c</sup> Includes mass of the radiator and reflector.

associated energy system. Consequently, the selection of the electric engine proved to be more difficult than the other cases.

We evaluated both the PPS 1350-G and the RIT-XT engines in simulated transfers to Mars. Differences in performance were found to be small, with an apparent advantage to the latter, and we end up deciding for the RIT-XT engine as the representative engine of the electric propulsion. Its main characteristics are shown in Table 1 (for a single RIT-XT engine, including the energy system).

Using the RIT-XT engine as baseline, we also briefly discuss the possible gains in performance if some future technologies would enhance the specific impulse or the thrust-to-weight ratio (see section 4.3). We considered a specific impulse and a thrust-to-weight ratio more than two times and three times the corresponding value of the RIT-XT engine, respectively. While the considered specific impulse increase would correspond to a direct technology enhancement in the engine, the increase in the thrust-to-weight ratio was based in foreseen developments in the energy system.

Another electrical propulsion technology that has been discussed for manned Mars missions is the magnetoplasmadynamic thruster (MPD) [17, 35]. The expected total thrust generated by these engines is orders of magnitude larger than the previously discussed electrical engines, even though the thrust-to-weight ratio and specific impulse is of the same order. However, the MPD that is claimed to have better results [17], explains that the engine could work only for about 1000 hours before degradation occurs [35], which is considerably less than the expected trip times. Furthermore, the  $F_T/w$  and  $I_{sp}$  values for the MPD are well within what we test for possible future technologies in section 4.3. Consequently, we decided not to explicitly consider MPD thrusters as continuous impulse engines in our study, although with the expected levels of thrust of these engines they could be considered to be in the frontier between impulsive and non-impulsive engines, and future studies should be performed (not only to increase the endurance time, but also to explore what can be achieved with this option).

#### 2.4. Nuclear Pure Electromagnetic Thrust

Propulsion technologies based on new concepts are constantly being proposed and tested. For instance, Electrodynamic Tethers, MagSails, Plasma Sails, and Solar Sails [11]. We included the Nuclear Pure Electromagnetic Thrust (PEMT) concept in our evaluation to see if such an advanced concept had

the potential for significantly reduce flight times for human missions to Mars. This engine uses the momentum of emitted photons, instead of expelling a working fluid to create thrust [13].

The thermal energy produced in a nuclear reactor is used to heat a radiator, which emits electromagnetic radiation (photons). The radiator is in front of a reflecting surface to direct the radiation that produces thrust. A Winston cone (Fig. 1), a non-focusing reflecting conical structure, can be used to collimate the radiation, resulting in a total thrust of  $F_T = W/c$ , where  $W$  is the power and  $c$  the speed of light [13].

The power emitted is related to the area of the surface of the radiator ( $S$ ) and its temperature ( $T$ ) through Stefan-Boltzmann's law, and the power produced by the nuclear engine. It is possible to ensure that a reasonable sized radiator yields say, 20 N, for a radiator temperature of about 3,300 K (close to the boiling point of a coolant). Among the materials that can withstand this radiator high temperature without melting, carbon nanotubes (as suggested by Rubbia), are the lightest [13]. The cone reflector must then envelop the radiator, and should have high reflectivity for the wavelength the radiator is emitting. For our radiator temperature, the reflector cone should be capable of reflecting visible and infrared radiation to be effective. Current technology for solar sails use composite booms (on the support structure) and Aluminised Mylar sails (or carbon fibre sail substrate), with densities of  $10 \text{ g/m}^2$  (including the support structure) [11]. Combining the densities of the materials and sizes of the structures, the radiator and reflector mass can be extracted (using the ideas of [13]).

As power source we have selected a NERVA-like reactor, resized and improved, as this is one of the discussed nuclear reactors with a power level closer to our intended figure. It is assumed a "NERVA 2000" reactor which can produce 22% more energy with an increase in mass of 26%, to get a net 20 N engine. The need for a nuclear reactor is justified by the  $50 \text{ km}^2$  of solar panels, weighting 44 kilotonnes, required to produce the same power using the already mentioned current technology [11, 27].

In the PEMT concept no mass is expelled. However, it is possible to determine its  $I_{sp}$ , to compare it with the propellant mass spent by chemical thrusters [13]. If we assume that the fraction of mass transformed into energy through nuclear fission is  $\xi = 10^{-3}$  [13], and it is ejected at the speed of light  $c$ , then the effective exhaust speed is  $v_{ex} = \xi c$ . Thus, the specific impulse is given by  $I_{sp} = 30,600 \text{ s}$ . The main features of the

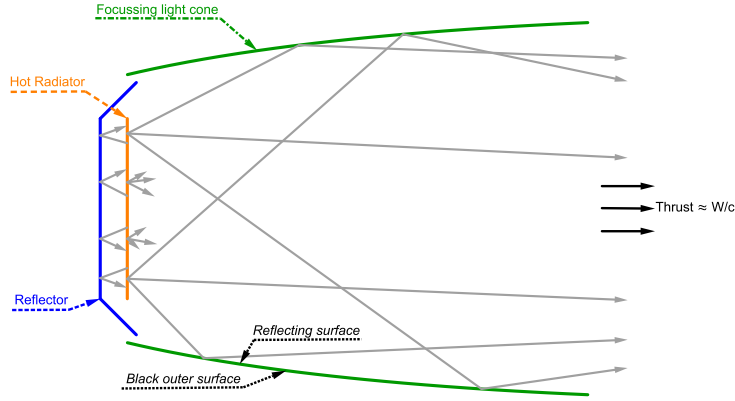


Figure 1: Scheme of Rubbia's engine concept [13]

engine are shown in Table 1.

The PEMT engine is, nevertheless, still a theoretical concept and present many potential difficulties to be implemented in practice: control of nuclear reactions in space (in free fall cooled only by radiation), insulation of the engine and the rest of the spacecraft, transfer of energy from the reactor to the radiator, etc. The required high temperature is another challenge since the radiator material must withstand it without melting. Some solutions such as discussed in [13] are somewhat difficult to implement. We nevertheless decided to include this technology, and use its optimistic characteristics at face value, to assess if such an engine proposal would offer some real advantages over other well known options.

### 2.5. Fuel Calculation

For engines that can be treated as impulsive, we consider the usual approximation of instantaneous change in velocity  $\Delta v$ , obtaining the propellant mass ( $M_P$ ) through the Tsiolkovsky rocket equation. The complete mission trajectory requires  $N$  manoeuvres that will be determined from the last to the first, since the fuel mass depends on the initial mass for each segment. The finite burn losses are taken into account by defining a loss factor [36].

For continuous thrust systems the spent fuel is determined at each instant by  $\dot{m} = -F_T/I_{sp}g_0$ , and taken into account in the numerical integration of the equations of motion.

In the case of PEMT, the fuel required is the nuclear material for the reactor, which is not expelled (it yields photons). Therefore, we need to compute the amount of nuclear material to load the reactor.

The thrust force of PEMT is given by the radiated power ( $W_{rad}$ ) divided by the speed of light ( $F_T = W_{rad}/c$ ) [13]. We assume that the radiated power is equal to the power generated by the reactor, i.e.  $W_{rad} = W_{reactor}$ . Combining this with the time of flight (ToF), which is equal to the operational time of the reactor,  $t_{on}$ , we compute the total burnup of the reactor,  $B = W_{reactor} \times t_{on}$ , expressed in  $\text{GW} \times \text{day}$  [13, 37].

The specific burnup,  $sb$ , of a nuclear material is the total energy released per unit of mass of nuclear fuel, and is expressed in  $\text{MW} \times \text{day}/\text{tonne}$  [38]. This is proportional to the

fractional burnup  $\beta$ , defined as the ratio of the number of fissions for a specified mass of fuel to the total number of heavy atoms [37]. Furthermore, if all fuel atoms were fissioned,  $\beta = 1$ , this would lead to  $950 \text{ GWd/t}$  for the uranium isotope  $^{235}\text{U}$  [37]. Consequently, the specific burnup is  $sb = 950\beta \text{ GWd/t}$ . Throughout our work we have used  $\beta$  equal to 4% [37, 38].

To determine the mass of uranium,  $M_U$ , required to produce the needed energy, we divide the total burnup obtained, by the specific burnup, i.e. we use  $M_U [\text{t}] = B [\text{GWd}]/sb [\text{GWd/t}] = W_{reactor} \times t_{on}/950\beta$ . If the nuclear reactor is loaded with uranium dioxide ( $\text{UO}_2$ ), enriched to almost weapon's level (80% of  $^{235}\text{U}$ ), using  $M_{\text{UO}_2} = M_U \times A_w^{\text{UO}_2}/A_w^{\text{U}}$  (where  $A_w^X$  is the atomic mass of element  $X$ ), we can compute the needed mass of uranium dioxide  $M_{\text{UO}_2}$  [39, 40, 37].

## 3. Mission to Mars

The mass and time required for a mission to Mars is dependent on its architecture. We consider a mission similar to the DRA 5.0 concept, that includes a manned spacecraft with a crew of four astronauts and an unmanned, or cargo, spacecraft.

The manned spacecraft is comprised of a human habitat module (which houses the crew during transit to and from Mars, and includes all life support systems for the mission), a propulsion system and a transport capsule. The first two might be assembled in orbit. The transport capsule carries the crew from low Earth orbit (LEO) to the main spacecraft on Earth, and between the main spacecraft and low orbit on Mars (upon arrival).

The unmanned cargo spacecraft consists of the propulsion system, the payload for Mars operations, including the descent and ascent vehicle, and the fuel required for the astronauts to return to the Earth, that will be transferred to the main spacecraft while in Mars orbit.

### 3.1. Mission Architecture & Mission Timeline

The same architecture is used to compare the performance of the different propulsion systems. Considering that the objective is to minimise the travel time for the astronauts, the crew

and most of the cargo are sent separately. This allows sending cargo through a slower and more economic way, reducing substantially the initial mass of the manned spacecraft.

The mission timeline for the manned phase is displayed in Fig. 2.

### 3.1.1. Parking Orbit & Departure

We have considered that the mission starts at LEO, where a launch system can deliver all the required modules for the mission. Both the main (manned) and the cargo spacecraft can be assembled at an initial circular parking orbit at about 500 km altitude, similar to the International Space Station, and which is high enough to allow assembly without decay.

After assembling and testing, the spacecraft would raise its apogee to an orbit with eccentricity 0.9, in a series of impulsive manoeuvres at perigee, so to minimise finite burn losses when compared to a direct interplanetary injection from LEO [36]. This saves mass by discarding the fuel tanks already used. The final elliptical orbit is selected to maximise its energy (but not too close to the escape energy to avoid complication with orbital perturbations and long periods of revolution). At the same time, we keep the perigee low to use the effectiveness of the Oberth effect when escaping from the Earth influence.

If continuous thrust (when applicable) would be used at departure, too much time would be required to escape, since the continuous thrust considered is yet of relatively small intensity. Therefore, we only considered chemical (or nuclear thermal if applicable) propulsion for escape and capture manoeuvres, and for the apogee raising initial manoeuvre. In this context, we considered several escape velocities  $v_\infty$  leading to different initial velocities for the interplanetary phase.

### 3.1.2. Interplanetary Transfer

The proximity of Mars implies that interplanetary transfer solutions with fly-by manoeuvres will increase the travel times making these uninteresting for the main spacecraft. For simplicity, we did not consider this option for the cargo mission as well. We are mainly interested in comparing the relative performance of the different propulsion systems and different, better options, for the cargo spacecraft can be used by all, improving all the considered alternatives equally. We also did not consider deep (impulsive) space manoeuvres as these are usually useful to synchronise with planets for fly-by, and they seem not to offer any advantage as compared with a larger  $\Delta v$  near the Earth (initial or final manoeuvre), due to the Oberth effect.

For the impulsive-type propulsion, chemical and nuclear thermal, once the initial velocity is defined a coast trajectory (Lambert arc) takes the spacecraft to the arrival planet, where it is captured. For the continuous thrust propulsion, electric and PEMP, the direction and intensity of the thrust can make a considerable difference and must be determined in each case to obtain a suitable solution. The continuous thrust can also be allowed to brake because it could imply a smaller requirement of propellant for the capture.

Our goal was not to completely optimise the trajectory, but to compare the relative performance of the propulsion systems.

### 3.1.3. Capture at Mars

The capture manoeuvre at Mars is performed using the classical single impulse brake, since continuous thrust brake would require too much time to execute for its level of thrust [13, 41, 9]. We also considered that aerobraking would be too dangerous for the manned spacecraft [42], and also would require shielding and a somehow compact and strong architecture, adding to the mass and losing part of its appealing (and possibly not compatible with a high area of solar panels in some options). Aerobraking, if one accepts the risk, requires a whole different analysis beyond the scope of this work.

The capture orbit, where the main spacecraft will be parked, has a periapsis altitude of 300 km, selected by comparison with other missions [43, 44, 45] and eccentricity 0.9. We selected this high energy orbit such that its low periapsis allows for an effective capture manoeuvre under high velocity, but minimising the fuel consumption during the capture. The main spacecraft is also used in the return trajectory and fuel is saved by not lowering the apoapsis. The fuel for the return trajectory is transported by the cargo spacecraft (sent previously and with the same capture orbit), and can now refuel the manned spacecraft for the return.

We did not consider *in situ* resource utilisation (ISRU), except for recycling of air and water (possibly included into the capsule), as our architecture is adequate for a fast first mission, and ISRU presents a new set of challenges. Apart from the risk, use of ISRU in a large scale to grow food and obtain mission support resources in general only makes sense for prolonged stays, which is not the case we are considering. The only remaining interesting use of ISRU is for generating return propellants. However, in the present case, they would have to ascend into orbit (with a 0.9 eccentricity), demanding more complex means of transportation than just bringing astronauts back. This would erode the advantage of ISRU, as the achieved gain in propellant mass would have to compensate a considerable increase in the mass of the transport vehicle, and the increase in propellant mass required to transport this vehicle to Mars. Therefore, it is not certain that ISRU would bring considerable advantages for the considered type of mission and, although its analysis is beyond the scope of this work, it remains an open issue.

Meanwhile the crew (using the transport capsule) would get all the required payload from the cargo spacecraft, and descend to a 300 km circular orbit. Afterwards, the crew changes to the Mars operations vehicle, that will descend to the surface, while the transport capsule waits in the circular orbit.

### 3.1.4. Return Trajectory

After completion of the ground operations, the crew ascends from the surface in the Mars operations vehicle (or part of it), returning to the transport capsule at low Mars altitude. After rendezvous and discard of the Mars operations vehicle, the transport capsule raises its orbit to return to the main spacecraft for the MtE (Mars to Earth) injection manoeuvre.

The capture at Earth is similar to the one at Mars (the entire spacecraft is captured and possibly reused; also, propulsion systems with nuclear material would have to be carefully decommissioned). Subsequently, the crew enters the transport ve-



Figure 2: Sketch of the manned mission timeline. Diamonds represent Single instants of time; rectangles, Mission phases; squares, Actions; oval shapes, Variable parameters (C3 equals the square root of the departure velocity)

hicle and returns to LEO where it will be transported back to Earth's surface.

A mission trade tree is displayed in Fig. 3, where we can see which propulsion system is used in each mission segment. When a coast transfer is selected no propulsion system is used during the interplanetary phase.

### 3.1.5. Cargo Mission Phase

Starting from the same assembly circular LEO, the cargo spacecraft raises the apogee altitude, similarly and for the same reasons than the manned spacecraft, to the same high elliptical orbit of eccentricity 0.9, and performs an EtM (Earth to Mars)

injection. Continuous propulsion could be used for this purpose advantageously. As the cargo spacecraft mass has mostly the same impact on the four discussed propulsion systems, we selected, without any adverse effects on the relative results, an impulsive (purely chemical) transfer approximated by a Hohmann transfer, for simplicity, and since a fast trajectory is not required for the cargo (the main goal is to minimise the required energy saving mass).

The cargo is to arrive at Mars before the crew, for the payload to be ready to descend to Mars. Upon arrival on Mars the capture of the cargo spacecraft to a highly elliptical orbit is similar to the manned spacecraft, since the latter will have to be



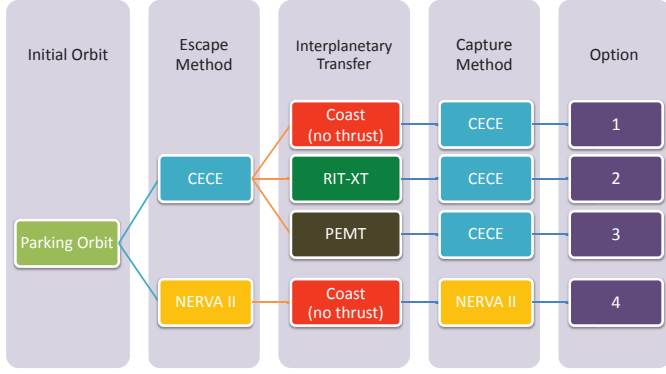


Figure 3: Different engine configurations assumed for the manned spacecraft

refuelled by the former to return to Earth.

### 3.2. Mass Budget

While crew, modules (habitat and cargo), and transport capsules remain constant, the type of propulsion and number of engines are variables of the problem. Propellants and tanks are also dependent on the execution time of the manoeuvres, since we considered different levels of finite burn losses [36]. The human habitat and cargo modules (including all necessary systems and payloads), and transport capsules, are an extrapolation from Mars Direct [1] and DRA 5.0 [3] concepts using typical guidelines [46].

The mass budget for the mission is therefore comprised of:

- Manned spacecraft (a fixed value including all systems and crew, except the propulsion system):  $M_{fixed}^{Manned} = 38$  t;
- Cargo spacecraft (again with exception of the propulsion system):  $M_{fixed}^{Cargo} = 42$  t;
- Mars operations vehicle (which will follow with the cargo spacecraft)  $M^{MOV} = 18$  t;
- Propulsion System,  $M_{PS}$ :
  - Impulsive engines (chemical or nuclear);
  - Continuous Thrust Engines, including:
    - \* Electric propulsion case: solar panels including structure, and power processing electronics;
    - \* Rubbia’s concept engine case: the radiator & reflector;
- Propellants,  $M_P^T$ ;
- Propellant tanks,  $M_T^T$ ;

The mass of the propellant tanks can be computed from the fuel mass (computed using the algorithm described in section 2.5), using a fitting function (from several specifications of existing tanks as input parameters [47]). Furthermore, they are sized in order to be empty and discarded after each large manoeuvre, as possible.

Consequently, the dry mass of the manned spacecraft is  $M_{Dry}^{Manned} = M_{fixed}^{Manned} + M_{PS}$ , where the tanks are not included since they are discarded after each manoeuvre. Its total mass is  $M_{Total}^{Manned} = M_{Dry} + M_P^T + M_T^T$ . The dry mass of the cargo spacecraft is  $M_{Dry}^{Cargo} = M_{fixed}^{Cargo} + M_{PS} + M_R^{FP}$ . The fuel payload entry ( $M_R^{FP}$ ) represents the propellants and tanks needed for the manned return trajectory. The total cargo mass is  $M_{Total}^{Cargo} = M_{Dry} + M_P^T + M_T^T$ .

Combining the total manned spacecraft mass for the Earth to Mars transfer, with the total cargo mass (which as mentioned above includes the return fuel for the manned spacecraft), yields the total mission mass ( $M_{Total} = M_{Total}^{Manned} + M_{Total}^{Cargo}$ ).

### 3.3. Trajectory Problem & Solution

To determine the trajectory and time of flight we adopt a simple patch-conic approximation [48], with a numerical integration in the interplanetary phase of the mission. We consider Earth and Mars to be in the same plane and in circular orbits around the Sun (with radius equal to the true semimajor axis). This makes the problem only dependent on the heliocentric angle between the planets and the characteristics of the mission, and not the specific launch date.

The spacecraft escapes from, and is captured into, an elliptical orbit with instantaneous manoeuvres at the periapsis of the orbits, using chemical or nuclear thermal propulsion. The terminal velocity,  $\vec{v}_\infty$ , of the escape hyperbola can make any angle with the velocity of the departure planet, within the planet’s orbital plane. The arrival velocity angle is determined by the interplanetary phase, a simple Lambert arc in the case of impulsive-type propulsion, or a trajectory determined by the continuous thrust that can include a brake segment to ease the capture manoeuvre.

A relatively simple approach is used to obtain a solution of the continuous thrust trajectory. Continuous thrust has a high  $I_{sp}$ , and the expense of propellant is not the main issue, so to minimise the transfer time the propulsion system works at full power [49, 34]. Consequently, only the direction of the thrust remains as a control parameter. A constant angle of the thrust with the instantaneous velocity vector (when accelerating and other for braking) is considered as being a compromise between a simple solution and the optimisation procedure used in [34]. This simple procedure does not assure a real optimal solution for a given mass of the mission, but it should be enough to compare the performance of the propulsion systems and determine an approximate time of flight.

The duration of operations on Mars is determined by the waiting time  $t_w$ . Our goal was to minimise the manned ToF, and ultimately the total duration of the manned part of the mission ( $t_{mission} = t_{EtM} + t_{MtE} + t_w$ ), and for a first exploration mission an extended time for operations is not required. The waiting time is determined by the time of flight of the EtM and MtE transfers, and depends critically on the heliocentric angle between the planets upon arrival at Mars. As we show on section 4, for all reasonable values of the parameters of the problem, it is impossible to avoid a prolonged stay on Mars.



### 3.4. Problem Parameters

Once the baseline mission is defined (including the mass budget), and settled what is transported to Mars, we focus on the objective of trying to minimise the ToF of the manned segment. For each propulsion system, the available thrust is increased by varying the number of engines employed.

As argued in [1] (the Mars Direct mission) a spacecraft with more than 1,000 t should be avoided. However, since we aim to test new propulsion systems and establish how fast we could reach Mars and get back (and since we are not completely optimizing the continuous thrust, and for simplicity use only impulsive thrust on the cargo spacecraft), we stretch the limit to 2,500 t for the whole mission (i.e. the sum of the manned and unmanned spacecraft). Without a mass limit, the mission could grow indefinitely with some ToF gains, but at a prohibitive cost.

We consider that the trajectory, and travel time, is defined by the following parameters:

1. Type of propulsion (see Table 1), considering different number of engines to increase total thrust;
2. Escape velocity on departure,  $\vec{v}_\infty$  (module and direction);
3. Thrust direction in the interplanetary phase, if applicable;
4. Brake location during the interplanetary phase (thrust direction after brake can be different than before);

For the chemical propulsion we consider a combination of two CECE engines as the unit propulsion system (i.e. the values of Table 1 multiplied by two). In the case of the NERVA engine the unit propulsion system is one engine. More engines can be added to increase the available thrust and thus avoid too long working periods (that leads to higher finite burn losses).

For the RIT-XT continuous propulsion engine we considered 5, 10, 15, 25, 35, 45, 60, 75, 100, 150, and 250 engines, because of its low thrust and mass. Nevertheless, we must remember that there is an associated energy system (that increases the mass), and that more thrust does not necessarily means a better performance. In the case of the PEMT concept, we only considered combinations of 1, 2, 3, and 4 engines due to its high mass.

For the escape velocity, we started with the one corresponding to the Hohmann transfer (HT) and searched for solutions with exponentially increasing values ( $v_\infty = [v_\infty^{HT} (1+0.02)^i]^2$ ,  $i = 0, 1, 2, 3, \dots, 200$ ). On the return transfer, we would in principle obtain retrograde interplanetary transfer orbits, when the value of  $\vec{v}_\infty$  is larger than the velocity of the planet. This case has no advantages relatively to the equivalent direct transfer, and it will not be considered.

Regarding the angles of both the escape velocity with the velocity of the planet ( $\theta_v$ ), and of the continuous thrust in the interplanetary phase (if applicable) with the velocity vector ( $\theta_{F_T}$ ), we consider values from  $0^\circ$  to  $-90^\circ$  with a  $-5^\circ$  step. The negative sign indicates that the velocity or thrust makes a retrograde angle with the velocity of the planet and the velocity of the spacecraft, respectively. We only considered negative angles as tests demonstrated that, all things equal, positive angles lead to worst performance, as expected [34].

Braking is defined as negative thrust in the considered direction, which is equivalent to a (positive) thrust at an angle  $180^\circ$

larger. Usually, reversing the thrust is only considered after the middle of the trajectory [34, 50, 51], but after testing we decided to consider that the reverse could occur at any of nine equally spaced radial distances between Earth and Mars.

## 4. Results & Discussion

### 4.1. Effects of Angle Variation and Direction

To better perceive the effect that  $\theta_v$  and  $\theta_{F_T}$  have on the system mass and ToF, we plotted the evolution of time versus mass, for an engine configuration and a single initial velocity (without brakes and for an one way trip).

In Fig. 4 we can see how a variation on the direction of the initial velocity (maintaining the same absolute value) result in variations of mass of the order of magnitude of the hundred tonne, and tens of days. For simplicity only the  $|\theta_v|$  variation are annotated in the figure, and only for an Earth to Mars transfer. The variation of  $\theta_{F_T}$  does not produce as strong effect as  $\theta_v$  here, although for  $|\theta_v| = 70^\circ$  some dispersion of the results can be seen (which is related with  $\theta_{F_T}$ ).

A closer analysis of the results reveals that the cause for the mass variation is the velocity on arrival. Through the change of the initial angle we induce a variation on the interplanetary ToF and, most importantly, a different spacecraft velocity vector when arriving at the target planet, affecting the arrival manoeuvre (and the required propellant), and hence every manoeuvre before that.

The fact that the thrust direction is not as important as the initial angle is explained by the relatively small continuous thrust considered in this situation. Higher thrust magnitudes induce a higher dispersion of results for the same initial velocity angle.

An interesting fact shown by Fig. 4 is the absence of higher values of  $\theta_v$ . For some values of the initial velocity and thrust magnitude, the spacecraft cannot reach the target planet when using high values of the initial velocity angle. A classical example of this is the Hohmann transfer, for which the only allowed angle for the initial velocity is zero.

Another aspect seen in Fig. 4 is that there are combinations of angles which yield missions with higher system mass and ToF (e.g. a mission with  $\theta_v = 0^\circ$  has a higher mass and ToF than one with  $|\theta_v| = 20^\circ$ ). As we aim to minimise both, these missions can be discarded. Therefore, for each escape velocity on departure we compute all  $\theta_v$  and  $\theta_{F_T}$  cases and select the best using a Pareto efficiency criteria (i.e. by ordering the cases in ascending order of time and then of mass, the points that show equal or higher times with higher masses are discarded).

Results show that most missions selected, as mention above, involve braking during the interplanetary phase (less than 2% do not include a brake), being more probable for the brake to start after the middle of the transfer, in accordance to the literature [34].

### 4.2. Chemical versus Nuclear Thermal propulsion

In the architectures we considered, an impulsive propulsion system is always required, as it is needed when performing

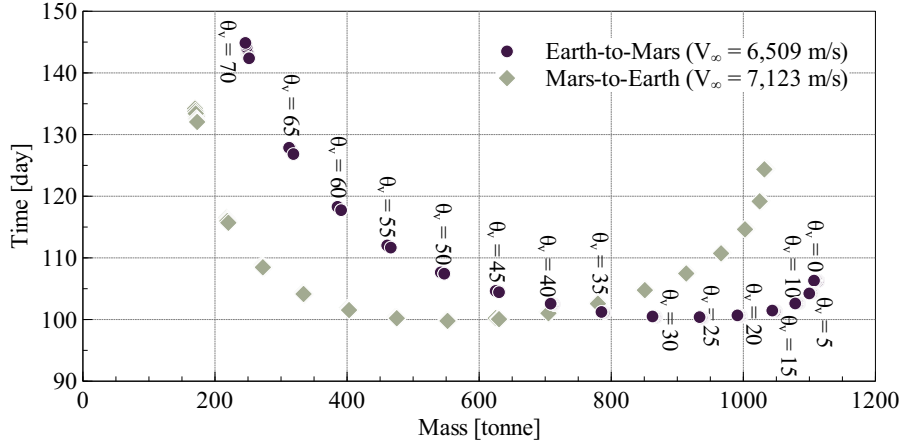


Figure 4: Interplanetary time of flight versus manned total spacecraft mass for ten RIT-XT engines, with constant initial velocity and multiple velocity and thrust angles

coast interplanetary transfers, or by the continuous thrust systems for the escape and capture manoeuvres (as explained in section 3.1). Therefore, the first test is to understand which of the systems (chemical or nuclear thermal) have a better mission performance for simple coast trajectories (since the continuous thrust may be seen as an addition to these solutions).

Results show that the pure chemical CECE propulsion system performs better than the nuclear thermal NERVA propulsion, for total mission masses lower than  $\sim 1,250$  t. Between about 1,250 t and about 1,600 t both options are fairly similar. Whereas, for total mission mass higher than about 1,750 t the NERVA system yields slightly better results (differences in mission mass of less than 22% of the total mission mass, for the same mission time).

Up to the mission mass order of magnitude for which the NERVA was designed for, about 1,000 t, the CECE smaller propulsion system mass outperforms the NERVA. Afterwards, the  $\sim 34$  t of the NERVA propulsion system represent less than 3.4% of the mission mass, and its higher  $I_{sp}$  and thrust start to have a positive impact on the total mission mass. These results also suggest that even if the performance could be enhanced as promised by the Phoebus proposal [25], no significant improvement would be achieved.

Considering these results, we only used chemical propulsion for departure and capture of the continuous thrust missions. Additionally, chemical propulsion has the advantage of being simpler, and more environmentally friendly, than nuclear propulsion [24, 52].

#### 4.3. Electric Engines

For the case of electric propulsion, we tested which configuration (in terms of number of engines) yields the best results. As the different engine configurations lead to similar outcomes we decided to determine which one has the lowest Pareto curve on average (for mission masses lower than our defined limit), using a trapezoidal integration. For the RIT-XT engine the configuration with lowest value involves 25 engines (although the

difference between the minimum and maximum values is very small).

We compare the selected RIT-XT engine with possible future technologies with increased specific impulse  $I_{sp}$  or thrust-to-weight ratio  $F_T/w$ , as explained in section 2.3. For the purposes of understanding the possible gains of such enhanced electric propulsion technology, we just computed the Earth to Mars transfer time of flight of the manned spacecraft. In each case we selected the best combination of electric engines (in terms of number of engines), resulting in the shortest ToF for the selected mass of the spacecraft. Results for a manned spacecraft with 1,000 t can be found in Table 2 and show that, although the considered values of specific impulse and thrust-to-weight of the enhanced technology are considerably larger, the performance change is marginal, and can even be degraded. The same result is obtained for other masses within the overall range of interest.

Our interpretation of these results is that continuous thrust is not the best choice of propulsion technology for the proposed goal of minimising the ToF for this architecture. Low intensity continuous thrust requires time to be effective, but to diminish the travel time is exactly the goal. As the technology improves, by improving the specific impulse or the thrust-to-weight ratio, the travel time diminishes, making the propulsion less effective and requiring more chemical fuel for the capture. This agrees with the existing literature: keeping the thrust-to-weight ratio constant and increasing the specific impulse increases the interplanetary transfer time while the interplanetary propellant mass decreases (i.e. changing the value of  $I_{sp}$  has a positive effect on the mass, but a negative one on the transfer time) [34]. Whereas the opposite effect for the transfer time and propellant mass is seen when the  $I_{sp}$  is fixed and the thrust-to-weight is increased [34]. The surprisingly small increase in performance suggests that large gains cannot be achieved even with future technological developments of the continuous propulsion. We therefore focus our analysis on the RIT-XT engine when comparing with other types of propulsion.

Table 2: Comparison of the time of flight to Mars using electric propulsion with increased specific impulse or thrust-to-weight (maintaining the remaining parameters of the engine constant, and for a wet mass at departure from Earth of the manned spacecraft of 1,000 t)

Case test	$F_T/w$ [N/kg]	$\frac{F_T/w}{(F_T/w)_{\text{RIT}}}$	$I_{sp}$ [s]	$\frac{I_{sp}}{(I_{sp})_{\text{RIT}}}$	No of engines	ToF [day]	$\frac{\text{ToF}}{(\text{ToF})_{\text{RIT}}}$
RIT-XT (baseline)	$4.3 \times 10^{-3}$	1	4,600	1	15	89.61	1
Larger $I_{sp}$	$4.3 \times 10^{-3}$	1	10,000	2.17	25	90.81	1.013
Larger $F_T/w$	$14.2 \times 10^{-3}$	3.3	4,600	1	75	89.26	0.996
Both $I_{sp}, F_T/w$ larger	$14.2 \times 10^{-3}$	3.3	10,000	2.17	250	89.16	0.995

#### 4.4. Nuclear Pure Electro-Magnetic Thrust

We expected the PEMT engine to perform better than the other studied propulsion technologies, as it has a much higher  $I_{sp}$  than any other engine. However, this technology has the disadvantage of a much higher permanent mass demanding much more from the auxiliary chemical propulsion for the capture. Fig. 5 plots the total manned mission time versus the total mass of the mission for different configurations, and it is explicit that for the allowed mission mass range only the one engine case is worth considering. Hence, we only compare the single PEMT engine case with the other technologies. Notice that the PEMT is a continuous thrust type engine and shares some of the disadvantages of the electric engines observed in section 4.3. A larger force, with the corresponding increase in engine mass, can be disadvantageous for the defined mass bounds because it requires more chemical propellants and deposits for the capture.

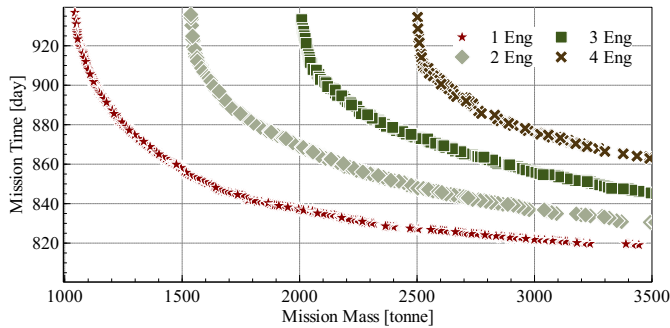


Figure 5: Mission total time versus mission total mass for the PEMT propulsion for different number of engines

#### 4.5. Systems Comparison

The results of total mission time and mass for the classical chemical solution, the nuclear thermal engine, 25 RIT-XT engines, and one PEMT, for several values of the initial escape velocity, are shown in Fig. 6. As can be seen, the electric systems give rise to the lowest curves (i.e. the lowest mass for the same ToF). The exception is for mission time higher than  $\sim 910$  days, where the simple classical chemical solution display similar outcomes (with differences less than 2% of total mission mass for the RIT-XT). Conversely, the system that shows higher mission masses is the PEMT, at least until about 1,500 t of total mission mass, from which the impulsive solutions have the worst results.

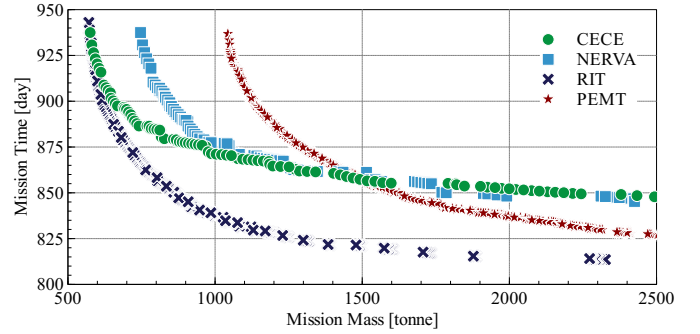


Figure 6: Total mission time (times of flight plus waiting time) versus total mission mass (manned plus cargo spacecrafts) for all systems configurations

Comparing the classical chemical solution with the 25 engines electric solution, we observe that adding to a largely optimised CECE system, a low mass and high  $I_{sp}$  system such as the electric propulsion, leads to improvements, in spite the limitations of the electric propulsion in increasing performance emphasised in section 4.3.

When using impulsive systems, given their low  $I_{sp}$ , an average of about 80% of the spacecraft mass is fuel (here including propellants and respective tanks to transport them), for this mass range. When adding the electric system this drops to about 75%, as the electric system is introduced not only for the spacecraft to reach its destination faster, but also for saving fuel by braking before arrival. Of this 75% fuel mass, only  $\sim 1\%$  corresponds to the electric system fuel.

Combining all EtM and MtE missions (as described in section 4.1), we determine the waiting time, total mission time and total mission mass. For the missions options presented in Fig. 6 the minimum waiting time achievable is  $\sim 520$  days (which corresponds to total mission times higher than  $\sim 900$  days). On the other extreme (total mission masses close to the 2,500 t limit and  $\lesssim 850$  days of mission time) the waiting time rises to  $\sim 570$  days, for continuous thrust options, and to about 660 days, for the classical chemical and nuclear thermal options. The classical options show waiting times consistently higher.

The waiting time evolution exposes its relation with travel time (and consequently the heliocentric angle). Even if we travel faster to Mars and back, the mission time is about the same, as the waiting time increases. Moreover, the waiting time is not only related to the travel time, but also with  $\theta_v$ , i.e. a different  $\theta_v$  requires the target planet to be in a differ-

ent rendezvous location, affecting the waiting time for the return. This reveals another advantage of using continuous thrust, the change in the velocity direction that can be imposed to the spacecraft. In many of these mission options the thrust is not aligned with the spacecraft velocity, but has a transverse component, which shortens the distance travelled, and affects the waiting time.

Comparing the mission outlined here (using 25 electric propulsion engines) with the Mars Direct mission [1], we show that it is possible to save about 50 days on the total mission time (and save  $\sim 60$  days on total ToF), while keeping the manned spacecraft below the 1,000 t limit as advocated in Mars Direct.

By contrast, there is no PEMT options with masses lower than 1,000 t, and only shows better results for masses higher than  $\sim 1,500$  t (the waiting time is almost 100 days lower than the chemical solution). The main reason for this is the way the engine generates energy. Since energy is generated through a nuclear reactor, which only burns 4% of the total nuclear material, the spacecraft is much heavier at arrival, requiring much more chemical propellant than other systems to be captured. For example, in an EtM transfer approximately 16.6 t of nuclear material is required for the interplanetary phase (ten times more than the electric option). Once the spacecraft reaches Mars the nuclear reactor still has  $\approx 16$  t of nuclear material (apart from the dry mass and fuel for the remaining transfers), which has to brake to be captured by Mars, whereas the electric option has already consumed all propellant and discarded its tanks (leaving it just with the dry mass and fuel for the remaining transfers). This has an exponential effect on previous manoeuvres and the required mass of the system. The option of getting rid of the PEMT engine after reaching Mars, and using another one that is already there to bring the crew back to Earth, is not considered due to the implied additional cost, the risk of discarding a large amount of nuclear fuel, and the increase in the mass to be transported that would make difficult for this options to be competitive.

For masses well above the considered limit, the PEMT ends up offering the best results (values not shown here). This might suggest that for trajectories to celestial bodies farther than Mars, where the engine would be operating during a longer period (and using the same mission architecture assumed here), the PEMT engine may turn out to be the best solution.

The total mission time is always large because even for the largest force and mission mass considered the ToF was never small enough that the heliocentric angle of the transfer would be larger than the heliocentric angle defined by the Earth during the transfer. Only then the waiting time could be small. When that does not happen any cut in the travel time will increase the waiting time.

Alternatively, instead of total mission time we could consider only the total travel time. This could be relevant if the astronauts could shelter themselves while at Mars, making pertinent just the time spent in space. Fig. 7 plots the total travel time — from Earth to Mars and return trip of the astronauts — against the total mission mass. In this case the classical chemical propulsion reveals to be the best, with NERVA being a very close second. When considering only the transfer times, it be-

comes clear that the advantage of the electric propulsion comes from saving mass and only stands because regarding impulsive types of propulsion, the faster they are the longer they have to wait in Mars. This result suggests that chemical propulsion would be the best to try to transfer to Mars before the opposition of Mars relative to the Earth, although a much larger mass than the considered in this work would be required.

## 5. Conclusions

We have shown that it is very difficult to significantly cut the duration of a mission to Mars, including the travel times (for this mission architecture). In fact, a reduction of an order of magnitude seems impossible with the foreseeable technologies and reasonable total mission mass, without using more exotic alternatives such as ISRU for fuel production or aerobraking. Moreover, the gains in travel time end up being lost in the additional required waiting time, so a significant improvement is not to be expected.

In the case of variable angle of thrust and use of continuous thrust in the cargo spacecraft an improvement in the total mass is to be expected but this would affect equally all options and a significant change is not foreseen.

The classical chemical propulsion gives the shortest heliocentric transfer times. In most cases, for the same total ToF, it has the smallest mass.

Electric propulsion offers some advantage, cutting the total mission mass (but not the travel time) but the advantages are limited, for the mission architecture assumed, since gains in the propulsion are lost when the travel time is cut. Our analysis suggests that an interesting combination might involve about twenty five engines. However, the interaction between them should be studied as suggested in [53].

The PEMT propulsion system revealed to be inadequate for a manned mission to Mars. The main reason is that it uses only a low fraction of the total nuclear material fuel for propulsion. If this fraction is increased, through technological improvements, the performance of the PEMT system can be greatly improved. Nevertheless, as it stands, the PEMT concept shows a better result for higher total mission mass values, suggesting that it may be more suitable for farther destinations than Mars.

## Acknowledgements

The work of Paulo J. S. Gil was supported by FCT, through IDMEC, under LAETA, project UID/EMS/50022/2013. The authors would like to thank John Brophy for helpful comments and suggestions on some issues of this manuscript.

## References

### References

- [1] R. Zubrin, R. Wagner, *The Case for Mars: the plan to settle the red planet and why we must*, The Free Press, New York, 1996.
- [2] D. Portree, *Humans to Mars: Fifty years of mission planning, 1950-2000*, Tech. rep., NASA History Division, Washington DC (2001).

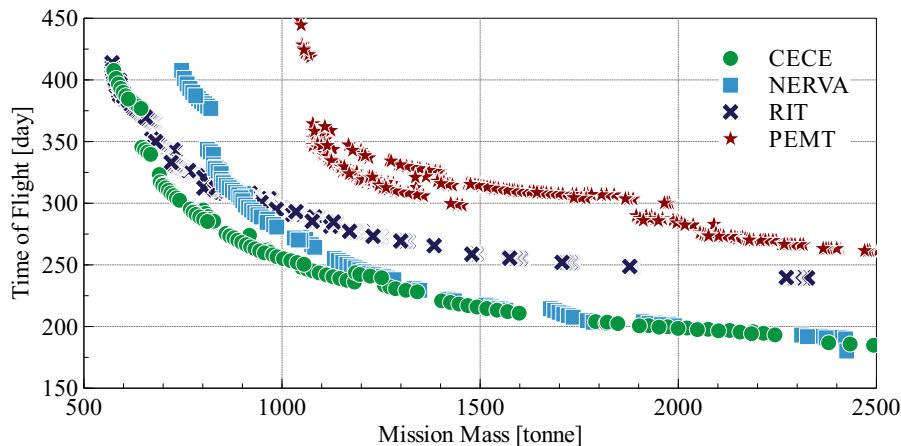


Figure 7: Total times of flight (Earth to Mars and return trip) for the astronauts as a function of the total mission mass

- [3] B. G. Drake, S. J. Hoffman, D. W. Beaty, Human exploration of Mars, Design Reference Architecture 5.0, in: 2010 IEEE Aerospace Conference, no.10, NASA Headquarters, IEEE, 2010, pp. 1–24. doi:10.1109/AERO.2010.5446736.
- [4] J. Vernikos, V. S. Schneider, Space, gravity and the physiology of aging: parallel or convergent disciplines? A mini-review, *Gerontology* 56 (2) (2010) 157–66. doi:10.1159/000252852.
- [5] F. A. Cucinotta, W. Schimmerling, J. W. Wilson, L. E. Peterson, G. D. Badhwar, P. B. Saganti, J. F. Dicello, Space radiation cancer risks and uncertainties for Mars missions, *Radiat. Res.* 156 (5) (2011) 682–688.
- [6] H. Price, A. Hawkins, T. Radcliffe, Austere Human Missions to Mars, in: AIAA SPACE 2009 Conference & Exposition, American Institute of Aeronautics and Astronautics, Reston, Virginia, 2009. doi:10.2514/6.2009-6685.
- [7] W. D. Woods, How Apollo Flew to the Moon, extended Edition, Springer, New York, 2011.
- [8] G. P. Sutton, O. Biblarz, Rocket Propulsion Elements, 7th Edition, John Wiley & Sons, New York, 2001.
- [9] S. Kemble, Interplanetary Mission Analysis and Design, Praxis Publishing, Berlin, 2006.
- [10] M. J. L. Turner, Rocket and Spacecraft Propulsion: Principles, Practice and New Developments, 3rd Edition, Springer Berlin Heidelberg, New York, 2008.
- [11] G. Vulpetti, L. Johnson, G. L. Matloff, Solar Sails: A Novel Approach to Interplanetary Travel, Copernicus Books, New York, 2008.
- [12] P. A. Czysz, C. Bruno, Future Spacecraft Propulsion Systems: Enabling Technologies for Space Exploration, 2nd Edition, Springer, Berlin, 2009.
- [13] C. Rubbia, Nuclear space propulsion with a pure electromagnetic thrust, Tech. rep., CERN, Geneva (2002).
- [14] O. Bertolami, M. Tajmar, Gravity control and possible influence on space propulsion: A scientific study, European Space Agency, ESA Publication Division, ESTEC, 2002, ESA CR(P) 4365.
- [15] M. Tajmar, O. Bertolami, Hypothetical Gravity Control and Possible Influence on Space Propulsion, *J. of Propuls. and Power* 21 (4) (2005) 692–696. arXiv:0412176, doi:10.2514/1.15240.
- [16] O. Bertolami, F. G. Pedro, Gravity Control Propulsion: Towards a General Relativistic Approach, *J. of the Br. Interplanet. Society* 60 (2006) 14. arXiv:0610116.
- [17] K. Sankaran, L. Cassady, a. D. Kodys, E. Y. Choueiri, A survey of propulsion options for cargo and piloted missions to Mars, *Annals of the New York Academy of Sciences* 1017 (2004) 450–467. doi:10.1196/annals.1311.027.
- [18] H. Oberth, Ways to Spaceflight, Tech. rep., National Aeronautics and Space Administration (1972).
- [19] EADS Astrium, Vinci Rocket Engine - Thrust Chamber, accessed 12 March 2012 (2012). URL <http://cs.astrium.eads.net/sp/launcher-propulsion/rocket-engines/vinci-rocket-engine.html>
- [20] Pratt & Whitney Rocketdyne, RL10B-2 (2009).
- [21] Pratt & Whitney Rocketdyne, Common Extensible Cryogenic Engine (CECE) (2009).
- [22] D. L. Black, L. H. Cooper, P. W. Dickson, J. S. Stefanko, C. Kim, Preliminary study of the NERVA II reactor design, Tech. rep., National Aeronautics and Space Administration (1964).
- [23] H. J. Leiter, R. Killinger, H. Bassner, J. Müller, R. Kukies, Development of the Radio Frequency Ion Thruster RIT XT - A Status Report, Tech. rep., Astrium GmbH, Munich (2001).
- [24] M. Klein, R. W. Schroeder, Nerva Program Requirements Document (1970).
- [25] D. Buden, Nuclear rocket safety, *Acta Astronautica* 18 (C) (1988) 217–224. doi:10.1016/0094-5765(88)90102-6.
- [26] J. C. Nance, Nuclear Pulse Propulsion, *IEEE Transactions on Nuclear Science* 12 (1). doi:10.1109/TNS.1965.4323511.
- [27] J. Brophy, R. Gershman, N. Strange, D. Landau, R. Merrill, T. Kerslake, 300-kW Solar Electric Propulsion System Configuration for Human Exploration of Near-Earth Asteroids, in: 47th AIAA/ASME/SAE/ASEE Joint Propulsion Conference & Exhibit, Joint Propulsion Conferences, American Institute of Aeronautics and Astronautics, 2011. doi:10.2514/6.2011-5514.
- [28] C. D. Brown, Elements of Spacecraft Design, American Institute of Aeronautics and Astronautics, Inc., Reston, VA, 2002.
- [29] Emcore Corporation, ZTJ Photovoltaic Cell Datasheet (2011).
- [30] J. W. Emhoff, I. D. Boyd, Modeling of Total Thruster Performance for NASA's Evolutionary Xenon Thruster Ion Optics, *J. of Propuls. and Power* 22 (4) (2006) 741–748. doi:10.2514/1.18975.
- [31] J. R. Brophy, M. G. Marcucci, G. B. Ganapathi, C. E. Garner, M. D. Henry, B. Nakazono, D. Noon, The Ion Propulsion System For Dawn, in: 39th AIAA/ASME/SAE/ASEE Joint Propulsion Conference and Exhibit, in Joint Propulsion Conferences, American Institute of Aeronautics and Astronautics, 2003, pp. 1–8. doi:10.2514/6.2003-4542.
- [32] C. Bundesmann, M. Tartz, F. Scholze, H. Leiter, F. Scortecci, D. Feili, P. E. Frigot, J. G. del Amo, H. Neumann, In-situ temperature, grid curvature, erosion, beam and plasma characterization of a gridded ion thruster RIT-22, in: 31st International Electric Propulsion Conference, IEPC, Ann Arbor, 2009, pp. 1–10.
- [33] Snecma, PPS 1350-G Stationary Plasma Thruster (2011).
- [34] A. Miele, Computation of Optimal Mars Trajectories via Combined Chemical/Electrical Propulsion, Part 1: Baseline Solutions for Deep Interplanetary Space, *Acta Astronautica* 55 (2) (2004) 95–107. doi:10.1016/j.actaastro.2004.01.053.
- [35] V. P. Ageyev, V. G. Ostrovsky, V. A. Petrosov, High-Current Stationary Plasma Accelerator of High Power, in: 23rd International Electric Propulsion Conference, Seattle, 1993, pp. 1071–1075.
- [36] C. D. Brown, Spacecraft mission design, 2nd Edition, American Institute of Aeronautics and Astronautics, Reston, VA, 1998.
- [37] J. R. Lamarsh, A. J. Baratta, Introduction to Nuclear Engineering, 3rd Edition, Prentice Hall, Upper Saddle River, 2001.
- [38] D. G. Cacuci, Handbook of Nuclear Engineering, Springer, London,

2010.

- [39] C. W. Forsberg, C. M. Hopper, J. L. Richter, H. C. Vantine, Definition of Weapons-Usable Uranium-233, Tech. Rep. March, Oak Ridge National Laboratory, Oak Ridge, Tennessee (1998).
- [40] R. D. Mosteller, Detailed Reanalysis of a Benchmark Critical Experiment: Water-Reflected Enriched-Uranium Sphere, in: Los Alamos National Laboratory (Ed.), Annual Meeting of the American Nuclear Society, Los Alamos, NM, 1994.
- [41] N. Calder, By Sun power to the Moon, Tech. Rep. June, European Space Agency, Noordwijk (2003).
- [42] J. L. H. Prince, R. W. Powell, D. Murri, Autonomous Aerobraking: A Design, Development, and Feasibility Study, *Advances in the Astronautical Sciences* 142.
- [43] K. Fletcher, Mars Express: The Scientific Investigations, Tech. rep., European Space Agency, Noordwijk (2009).
- [44] S. Maurice, W. Feldman, B. Diez, O. Gasnault, D. J. Lawrence, a. Pathare, T. Prettyman, Mars Odyssey neutron data: 1. Data processing and models of water-equivalent-hydrogen distribution, *Journal of Geophysical Research* 116 (E11) (2011) E11008. doi:10.1029/2011JE003810.
- [45] J. E. Graf, R. W. Zurek, H. J. Eisen, B. Jai, M. Johnston, R. DePaula, The Mars Reconnaissance Orbiter Mission, *Acta Astronautica* 57 (2-8) (2005) 566–578. doi:10.1016/j.actaastro.2005.03.043.
- [46] P. Fortescue, J. Stark, G. Swinerd, *Spacecraft Systems Engineering*, 4th Edition, Wiley, Hoboken, N.J, 2011.
- [47] ASTRION Space Transportation, Propellant Tanks for Spacecraft (2010).
- [48] R. R. Bate, D. D. Mueller, J. E. White, *Fundamentals of Astrodynamics*, Dover Publications, New York, 1971.
- [49] C. L. Ranieri, C. A. Ocampo, Indirect Optimization of Three-Dimensional Finite-Burning Interplanetary Transfers Including Spiral Dynamics, *J. of Guidance, Control, and Dynamics* 32 (2) (2009) 445–455. doi:10.2514/1.38170.
- [50] L. Derosa, C. Maccone, Propulsion tradeoffs for a mission to Alpha Centauri, *Acta Astronautica* 60 (8-9) (2007) 711–718. doi:10.1016/j.actaastro.2006.10.003.
- [51] B. A. Conway (Ed.), *Spacecraft Trajectory Optimization*, Cambridge University Press, New York, 2010.
- [52] The Planetary Society, Nuclear Space Initiative: A Planetary Society White Paper (2005).  
URL [http://www.planetary.org/action/opinions/nuclear\\_propulsion\\_0505.html](http://www.planetary.org/action/opinions/nuclear_propulsion_0505.html)
- [53] National Aeronautics and Space Administration, NASA’s Evolutionary Xenon Thruster (2008).